Chemical Abundances in the Universe:
Connecting First Stars to Planets
Proceedings IAU Symposium No. 265, 2009
K. Cunha, M. Spite & B. Barbuy, eds.

doi:10.1017/S1743921310000657

Haro15: Is it actually a low metallicity galaxy?

Verónica Firpo[1], Guillermo Bosch[1], Guillermo Hägele[1,2], Ángeles I. Díaz[2], and Nidia Morrell[3]

[1]Facultad de Ciencias Astronómicas y Geofísicas, Universidad Nacional de La Plata, Paseo del Bosque s/n, B1900FWA, La Plata, Argentina.
email: vfirpo@fcaglp.unlp.edu.ar

[2]Departamento de Física Teórica,C-XI, Universidad Autónoma de Madrid, Spain.

[3]Las Campanas Observatory, Carnegie Observatories, La Serena, Chile.

Abstract. We present a detailed study of the physical properties of the nebular material in multiple knots of the blue compact dwarf galaxy Haro 15. Using long slit and echelle spectroscopy, obtained at Las Campanas Observatory, we study the physical conditions (electron density and temperature), ionic and total chemical abundances of several atoms, reddening and ionization structure. The latter was derived by comparing the oxygen and sulphur ionic ratios to their corresponding observed emission line ratios (the η and η' plots) in different regions of the galaxy. Applying direct and empirical methods for abundance determination, we perform a comparative analysis between these regions.

Keywords. (ISM:) H II Regions, starburst, Haro 15, abundances.

Observations

We obtained high dispersion (Echelle Spectrograph; $\Delta\lambda$= 0.148Å px^{-1} at 5400Å equivalent to 6.72 kms^{-1}px^{-1}) and long-slit low resolution spectra (WFCCD; $\Delta\lambda$= 4.2Å px^{-1} at 5400Å) of five luminous knots in the BCD galaxy Haro 15 (Fig. 1) at the du Pont Telescope. We have obtained a good flux calibration in both groups of data and we can confirm that the two different data groups are comparable in knot B and C.

Electron density and temperatures

We have followed the same procedure described in detail in Hägele *et al.* (2006), (2008), Hägele (2008) to derive the physical properties of the nebular material in the observed regions. The [OIII] λ 4363Å auroral emission line is only detected in knot B (longslit and echelle) and knot C (longslit). It was only possible to derive T[OIII], T[SIII], T[OII] and T[SII] from direct measurements for knot B. For the other knots, for which we are not able to measure some lines such as [OII] $\lambda\lambda$ 3727Å, [SIII] $\lambda\lambda$ 9069,9532Å or auroral lines, we have resorted to models that predict relationships between emission lines for different temperatures, for example the relation between T[OII] and T[OIII] found by Pérez-Montero & Díaz (2003). In the case of densities, the knots show density values in the low density limit (ne $<$ 100cm^{-3}), typical for of this kind of objects, with the exception of knot E (ne $\approx$ 280cm^{-3}).

Chemical Abundances: O, S, N, Ar, Ne

Oxygen abundances and their uncertainties were derived for each observed knot using the direct method, where it could be applied, or several empirical methods using the strong emission lines present in the spectra. We notice a difference in the O/H ratio between knots A and B. This difference was suggested by López-Sánchez & Esteban (2009) as the two objects might have had a different chemical evolution. Our results support these differences between the two regions. Knot C shows oxygen abundance

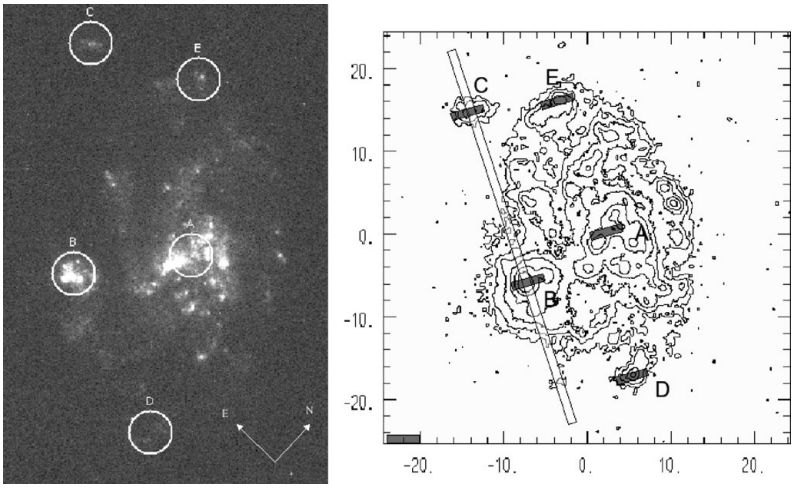

Figure 1. Left panel: HST archive image showing the location of the observed regions. Right panel: Contour maps of the continuum-subtracted Hα image (Cairós *et al.* 2001). In this image we show the slits distribution. The long-slit spectroscopy (1" wide) can be seen running through Haro15-B and Haro15-C. Five pointings were observed with the echelle mode, shown as dark rectangular (1"x4") slits.

similar to that of knot B, while the oxygen abundance derived for knot E is closer to the abundance calculated for knot A. The S/N in our knot D spectra is not as good as for the other knots, and the quantities derived for this region should be used with caution.

In the cases that we can use the direct method, the total abundances have been derived taking into account the unseen ionization stages of each element, resorting to the most widely accepted ionization correction factors (ICF) for each species [X/H=ICF(X^{+i}) * (X^{+i}/H^{+})] (see Pérez-Montero *et al.* 2007, Hägele *et al.* 2008). The N and Ar abundances are higher in knot A than in knot B, although the S abundance derived for knot A lies between those derived from echelle and longslit of knot B.

Ionization Structure

The ratio between O^{+}/O^{2+} and S^{+}/S^{2+} denoted by η is intrinsically related to the shape of the ionizing continuum and depends on nebula geometry only slightly (Vílchez & Pagel, 1988). We can include knot B in this diagram, lying in the highest excitation region. The purely observational counterpart, the η' diagram (η'=[([OII]/[OIII])/([SII]/[SIII])), where η and η' are related through the electron temperature but very weakly. The position of knot B in both diagrams shows a compatible ionization structure.

References

Hägele, G. F., Pérez-Montero, E., Díaz, A. I., Terlevich, E. and Terlevich, R.2006, *M.N.R.A.S.*, 372, 293-312

Hägele, G. F., Díaz, A. I., Terlevich, E., Terlevich, R., Pérez-Montero, E. and Cardaci, M. V. 2008, *M.N.R.A.S.*, 383, 209-229

Hägele, G. F. 2008, PhD Thesis at Universidad Autónoma de Madrid, *arXiv*, 0908.4285v1

López-Sánchez A. R. & Esteban C., 2009 *arXiv*, 0910.1578

Pérez-Montero E. & Díaz A. I., 2003 *M.N.R.A.S.*, 346, 105

Pérez-Montero, E., Hägele, G. F., Contini, T., & Díaz, Á. I., 2007 *M.N.R.A.S.*, 381, 125

Vílchez J. M. & Pagel B. E. J., 1988 *M.N.R.A.S.*, 231, 257

Cairós, L. M., Caon, N.,Vílchez, J. M., González-Pérez, J. N., & Muñoz-Tuñón, C., 2001 *ApJS*, 136, 393